Hydrology and Earth System Sciences Discussions

Baseflow simulation of SWAT model in an inland river basin in Tianshan Mountains, Northwest China

Y. Luo[1,2], J. Arnold[3], P. Allen[4], and X. Chen[1]

[1]State Key Laboratory of Desert and Oasis Ecology, Xinjiang Institute of Ecology and Geography, Chinese Academy of Sciences (CAS), China
[2]Key Laboratory of Ecosystem Network Observation and Modeling, Institute of Geographic Sciences and Natural Resources Research, CAS, China
[3]Grassland Soil and Water Research Laboratory, USDA-ARS, Temple, Texas 76502, USA
[4]Department of Geology, Baylor University, Waco, Texas 76798, USA

Correspondence to: Y. Luo (luoyi.cas@hotmail.com)

Abstract

Baseflow is an important component in hydrological modeling. Complex streamflow recession process complicates the baseflow simulation. In order to simulate the snow and/or glacier melt dominated streamflow receding quickly during high-flow period but very slowly during the low-flow period in rivers in arid and cold Northwest China, the current one-reservoir baseflow approach in SWAT (Soil Water Assessment Tool) model was extended by adding a slow reacting reservoir and applied to the Manas River basin in Tianshan Mountains. Meanwhile, a digital filter program was employed to separate baseflow from streamflow records for comparisons. Results indicated that the two-reservoir method yielded much better results than the one-reservoir one in re-producing streamflow processes, and the low-flow estimation was improved markedly. Nash-Sutcliff efficiency values at the calibration and validation stages are 0.68 and 0.62 for the one-reservoir case, and 0.76 and 0.69 for the two-reservoir case, respectively. The filter-based method estimated the baseflow index as 0.60, while the model-based as o.45. The filter-based baseflow responds almost immediately to surface runoff oc-currence at onset of rising limb, while the model-based with a delay. In consideration of watershed surface storage retention and soil freezing/thawing effects on infiltration and recharge during initial snowmelt season, a delay response is considered to be more reasonable. However, a more detailed description of freezing/thawing processes should be included in soil modules so as to determine recharge to aquifer during these processes, and thus an accurate onset point of rising limb of the simulated baseflow.

1 Introduction

Baseflow is a streamflow component which reacts slowly to rainfall and is usually asso-ciated with water discharged from groundwater storage (Eckhardt, 2008). Knowledge about baseflow is useful in assessing water quality, forecasting streamflow, allocat-ing water supply, and designing hydropower plant (Tallaksen, 1995) under low-flow

conditions. When, where, and how much streamflow can be attributed to groundwater discharge are thus practically important.

Baseflow is, therefore, an important component in hydrological simulation. Conceptual modeling of baseflow usually assumes that outflow from the aquifer is linearly proportional to its storage (Aizen et al., 2000; Fenicia et al., 2006; Eckhardt, 2008; Ferket et al., 2010), sometimes combined with analytical solutions of the simplified Boussinesq equation (Paniconi et al., 2003; Troch et al., 2004; Hilberts et al., 2004). Wittenberg (1999) argued that the unconfined aquifer is unlikely a linear reservoir, instead, more likely an non-linear one. However, Fenicia (2006) confirmed that the linear storage-discharge relationship describes best of the groundwater behavior. Baseflow itself may be composed of a number of components, each of which may vary seasonally with different recession constant (Nathan and McMhon, 1990). As probably a comprise, multi-reservoir algorithms, linear, non-linear, or combined were tried to generate baseflow by, e.g., Tallaksen (1995), Ferket et al. (2010), and Samuel et al. (2011).

Soil Water Assessment Tool (SWAT, Arnold and Fohrer, 2005) uses a conceptual linear one – reservoir (shallow aquifer storage) approach to simulate baseflow. SWAT partitions groundwater into two aquifer systems: a shallow aquifer which contributes baseflow to streams within the watershed, and a deep aquifer which contributes baseflow to streams outside the watershed and can be considered lost from the system (Arnold et al., 1993). While the shallow aquifer – baseflow was properly reproduced by SWAT (Arnold et al., 2000; Jha et al., 2007), weaker simulation of baseflow was found as well (Kalin and Hantush, 2006; Srivastva et al., 2006). Peterson and Hamlett (1998) found that SWAT was not able to simulate baseflow due to the presence of soil fragipans. Chu and Shirmohammadi (2004) found that the base flow was not simulated properly for an extremely wet year. Wu and Johnston (2007) found underestimated baseflow by SWAT especially during dry years in a Great Lake watershed and indicated that this is due primarily to the long temporal lag between winter snowpack accumulation and spring snow melting events. Luo et al. (2011) found underestimation of baseflow in during the low-flow period in the Manas River Basin in Northern

Tianshan Mountains using the SWAT2005. For the glaciated Oigaing River basin in Western Tianshan and the Ala Archa River basin also in Northern Tianshan, Aizen et al. (2000) used one linear reservoir to generate baseflow and found that the discharge was underestimated during autumn-winter time as well. The steep slopes of the river basins in Tianshan Mountains, the quick recession of surface runoff, and the sluggish and stable baseflow processes might indicate a quick percolation of rainfall and snow and glacier melt waters during the summer time to an underground storage which releases slowly during the winter time. Nathan and McMhon (1990) indicated that baseflow itself may be composed of a number of components, each of which may vary seasonally with different recession constant. Supposedly, an additional slow release pool may improve the low-flow estimation for rivers in Tianshan Mountains, which is not present in both Aizen's (2000) model and SWAT model.

Therefore, the main objective of the paper is to develop a two-reservoir approach for baseflow simulation in SWAT and use the model to simulate the streamflow process that is characterized by *combined steep and sluggish recession stages of the receding limb* in an arid and cold inland river basin in Tianshan Mountains, Northwest China.

2 Materials and methods

2.1 Baseflow modeling in SWAT

In SWAT model, water routed through channel system to the gauges consists of four components, direct surface runoff (Q_{sf}), lateral flow from unsaturated soil profiles (Q_{lt}), drainage from tiles (Q_{tl}), and baseflow from underground storage (Q_b), Fig. 1. Modeling of the direct surface runoff, the lateral soil flow, and the tile drainage are detailed in theoretical documents of SWAT model (Neitsch et al., 2005) and thus, will not be described repeatedly here. The baseflow simulation will be focused hereafter.

SWAT differentiates the underground storage into two portions, shallow aquifer and deep aquifer. The shallow aquifer receives recharge from the unsaturated soil profile percolation. An exponential decay weighting function is utilized to account for the time delay in aquifer recharge once the water exits the soil profile (Neitsch et al., 2005). The delay function accommodates situations where the recharge from the soil zone to the aquifer is not instantaneous, i.e. 1 day or less. The recharge to aquifer on a given day is calculated as below:

$$W_{rchrg,i} = \left[1 - \exp\left(-\frac{1}{\delta_{gw,sh}}\right)\right] W_{seep} + \exp\left(-\frac{1}{\delta_{gw,sh}}\right) W_{rchrg,i-1} \tag{1}$$

where W_{rchrg} is the amount of recharge entering the aquifers (mm H_2O day^{-1}), $\delta_{gw,sh}$ is the delay time of the overlying geologic formations (days), W_{seep} is the total amount of water exiting the bottom of the soil profile (mm H_2O day^{-1}); subscriptions seep indicates seepage water exiting bottom of unsaturated soil profile, rchrg indicates recharge, i is the sequential number of days, and sh indicates the shallow aquifer storage.

A fraction of the total daily recharge can be routed to the deep aquifer. The amount of water then will be diverted from the shallow aquifer due to percolation to the deep aquifer on a given day is given by:

$$W_{seep,dp,i} = \beta_{dp} W_{rchrg,i} \tag{2}$$

where β_{dp} is a coefficient of shallow aquifer percolation to deep aquifer, and subscription dp indicates deep aquifer.

The amount of recharge entering the shallow aquifer is:

$$W_{rchrg,sh,i} = W_{rchrg,i} - W_{seep,dp,i} \tag{3}$$

Baseflow generated from the shallow aquifer on a given day i under influence of recharge is given as below (Neitsch et al., 2005):

$$Q_{b,sh,i} = Q_{b,sh,i-1} \cdot \exp\left(-\alpha_{gw,sh} \cdot \Delta t\right) + W_{rchrg,sh,i} \cdot \left[1 - \exp\left(-\alpha_{gw,sh} \cdot \Delta t\right)\right] \tag{4}$$

Printer-friendly Version

Interactive Discussion

where $Q_{b,sh,i}$ is the baseflow from the shallow aquifer on day i (mm H$_2$O day^{-1}), and b indicates baseflow, and Δt is the step time length. Daily time step is used in this study.

When only one reservoir is used, the baseflow is equal to that from the shallow aquifer.

$$Q_{b,i} = Q_{b,sh,i} \tag{5}$$

SWAT assumes that water enters the deep aquifer is not considered in the future water budget calculations and can be considered lost from the system (Neitsch et al., 2005). This study uses the deep aquifer as a parallel reservoir generating the baseflow, which enters the channel system eventually, to improve the streamflow process simulation in the low-flow period. When two – reservoir approach is used, baseflow from the shallow aquifer is expressed as in Eq. (4), and following Eqs. (1) and (2), the recharge to and baseflow from the deep aquifer are given by Eqs. (6) and (7), respectively.

$$W_{rchrg,dp,i} = W_{rchrg,dp,i-1} \cdot \exp\left(-\frac{1}{\delta_{gw,dp}}\right) + W_{seep,dp,i} \cdot \left[1 - \exp\left(-\frac{1}{\delta_{gw,dp}}\right)\right] \tag{6}$$

$$Q_{b,dp,i} = Q_{b,dp,i-1} \cdot \exp\left(-\alpha_{gw,dp} \cdot \Delta t\right) + W_{rchrg,dp,i} \cdot \left[1 - \exp\left(-\alpha_{gw,dp} \cdot \Delta t\right)\right] \tag{7}$$

where $W_{rchrg,dp}$ is the amount of recharge entering the deep aquifer (mm H$_2$O day^{-1}), $\delta_{gw,dp}$ is the delay time or drainage time of the deep aquifer geologic formations (days), $W_{seep,dp}$ is the total amount of water exiting the bottom of the shallow aquifer (mm H$_2$O day^{-1}), $Q_{b,dp}$ is baseflow component from deep aquifer. Total baseflow is then given as below:

$$Q_{b,i} = Q_{b,sh,i} + Q_{b,dp,i} \tag{8}$$

when the shallow storage reservoir is used only to generate baseflow, recharge to the deep aquifer is disabled. When both aquifers are used to generate baseflow, the parameter β_{dp} will be determined through calibration. Other parameters to be calibrated for baseflow modeling include the delay time $\delta_{gw,sh}$, $\delta_{gw,dp}$, and the recession constants $\alpha_{gw,sh}$ and $\alpha_{gw,dp}$.

2.2 Baseflow separation using automated digital filter

In consideration of difficulties in measurement of baseflow, a third-party approach, the digital filter-based program is used to separate baseflow from streamflow records for comparison purposes. This baseflow separation procedure is based on a recursive digital filter commonly used in signal analysis and processing (Lyne and Hollick, 1979) and used, among others, by Nathan and McMahon (1990), Arnold and Allen (1999), Szilagyi et al. (2003), Szilagyi (2004), and Eckhardt (2005, 2008). This technique is in fact just arbitrary and physically unrealistic, however, it does provide subjective and repeatable estimate of baseflow that is easily automated (Nathan and McMahon, 1990). The filter is given as below:

$$Q_{\text{sf},i} = \lambda Q_{\text{sf},i-1} + \frac{1+\lambda}{2}\left(Q_{\text{s},i} - Q_{\text{s},i-1}\right) \tag{9}$$

where Q_{sf} and i are defined as before, Q_{s} is the surface runoff, and λ is the filter parameter. Baseflow is calculated as below:

$$Q_{\text{b},i} = Q_{\text{s},i} - Q_{\text{sf},i} \tag{10}$$

where Q_{b} is defined as before.

An automatic baseflow filter program (Arnold et al., 1995, http://swatmodel.tamu.edu/software/baseflow-filter-program, 2011) is used to separate baseflow from the daily streamflow records from 1961 to 1999 in Manas River Basin (MRB).

2.3 Watershed and data description

2.3.1 Model setup

MRB is located at northern side of the middle Tianshan Mountains, Northwest China, Fig. 2. MRB originates from the Yilianhabierga Mountain, runs 160 km to the outlet at Kenswat Hydrological Station (KHS, 85°57′ E, 43°58′), and runs further 240 km through

the oasis and the desert and finally merges into the Manas Lake. Catchment area of the MRB above the outlet KHS is 5163 km^2.

Maps of a 1 : 250 000 DEM, a 1 : 100 000 land cover, and the China Glacier Inventory (CGI) were used to setup the ArcSWAT2005. The CGI data used as initial glacier layout were mainly derived from topographical maps (1 : 100 000) based on aerial photos acquired during 1962–1977 (Shangguan et al., 2009). Eventually, the watershed is delineated into 27 subbasins and 163 Hydrological Response Units (HRUs). Each subbasin was divided into ten bands with equal elevation increment for simulating the snow and glaciers.

(1) Topography and land covers

Altitude of the MRB ranges from 858 meters above sea level (m a.s.l.) to 5146 m a.s.l. Physical features of the subbasins and glaciers in each subbasin are listed in Table 1. Differences of elevation within a subbasin are significant. On average, the difference is 2561 m, with the biggest 3876 m for the subbasin 11 and the smallest 448 m for the subbasin 1. The land cover types include the range grassland of 8.11 % within the elevation band 2500–3500 m a.s.l., short bushes of 39.1 % within the elevation band of 1500–2500 m a.s.l., and forest of 5.32 % within the below the elevation of 1500 m a.s.l., the bare land of 33.58 %, and glaciers. Among the 163 HRUs, there are 28 glacierized ones with total glacier area of 717 km^2. Ratios of glacier area to subbasin area range from 0.7 % for the subbasin 4 to 51.2 % for the subbasin 22, with a mean ratio of 13.9 % over the basin. Watershed glacier processes simulation was detailed in Luo et al. (2011, manuscript).

(2) Soils

Main soils in the basin include alpine meadow soil, subalpine meadow soil, subalpine meadow and steppe soil, mountain chernozem soil, mountain grey cinnamon soil, mountain chestnut soil, which take account of 36 %, 11 %, 42 %, 1 %, 7 %, and 3 %

of the basin area, respectively. Textures and properties of these soils were derived from the field collected and lab tested data of the publication "Soils in Xinjiang (unpublished)".

(3) Climate

The Shihezi Weather Station (SWS, N 43°29′, E 87°06′) is located below the outlet with an elevation of 444 m a.s.l. The daily meteorological data include maximum and minimum temperatures, wind speed at 10 m height, relative humidity, precipitation, and 20 cm-pan evaporation from 1961 to 1999. This area displays alpine climate, very cold winter and moderate summer temperatures. The mean high temperature is 39.6 °C, the low −31.7 °C, and the daily average 7.0 °C. The mean annual precipitation is 196 mm and the pan evaporation 1714 mm.

For each subbasin, a virtual weather station (VWS) is defined. For each VWS, the temperature and precipitation data were derived from the SWS by using the temperature and precipitation lapse rates. Default value −6 °C km^{-1} in SWAT model was used for the temperature lapse rate, and 45 mm km^{-1} was used for the precipitation lapse rate (Luo et al., 2011, manuscript).

(4) Streamflow

Daily streamflow records at the KHS from 1961–1999 were used. The mean daily discharge rate is 39.3 m^3 s^{-1} and the average annual volume 12.15 × 10^8 m^3. The recorded maximum annual volume is 20.08 × 10^8 m^3 in 1999 and the minimum 9.39 × 10^8 m^3 in 1983. The flow volume from June to August takes account of 70.5 % of the annual value and of 28.9 % and 25.9 % for July and August, respectively. During the seven months from October to the next April, flow volume accounts for 15.9 % of the year with the monthly ratio decreasing from 4.2 % in September to 1.2 % in February and then going up gradually to 2.0 % in April.

MRB is snow and glacier melt dominated. Snowmelt starts usually at late April or early May, glacier melts as snowpack depletes, and streamflow starts to rise consistently till peak discharge at late July. Glacier melt contribution ceases at late September. As temperature falls below 0 °C, a new snowpack season begins, and the direct surface runoff to streamflow ceases. Steep rising and receding streamflow curve is then followed with a almost flat low-flow line during the Winter and Spring seasons, while the streamflow is very stable and has a quite long duration, Fig. 3, which is a common feature of the river flows in Northwest China.

The daily streamflow dataset was split into two segments from 1961 to 1980 and from 1981 to 1999 for calibrating and validating the SWAT model, respectively. The simulated streamflow was compared to the measured values on the daily basis and the model performance was evaluated using both Nash-Sutcliffe efficiency (NSE) and Percent Bias (PBIAS) indices (Moriasi et al., 2007).

$$NSE = 1 - \frac{\sum_1^n \left(Q_i^{obs} - Q_i^{sim}\right)^2}{\sum_i^n \left(Q_i^{sim} - Q^{mean}\right)^2} \tag{11}$$

$$PBIAS = \frac{\sum_1^n \left(Q_i^{obs} - Q_i^{sim}\right)}{\sum_i^n Q_i^{obs}} \times 100 \tag{12}$$

where Q_i^{obs} is the ith observation for the daily flow, Q_i^{sim} is the ith simulation value for the daily flow, Q^{mean} is the mean of observed data for the daily flow, and n is the total number of the daily flow observations.

NSE indicates how well the plot of observed versus simulated data fits the 1 : 1 line. NSE ranges between $-\infty$ and 1.0 (1 inclusive), with NSE = 1 being the optimal value. PBIAS measures the average tendency of the simulated data to be larger

or smaller than their observed counterparts. The optimal value of PBIAS is 0.0, with low-magnitude values indicating accurate model simulation (Morasi et al., 2007).

3 Results

Parameters calibrated for baseflow components are listed in Table 1 for reference. In case one-reservoir was used only, it was assumed that water exiting bottom of the un-saturated soil profiles recharged the shallow aquifer only. When two-reservoir method was employed, it was found that 40 % of recharge to the deep aquifer was proper to match the measured streamflow during low-flow period. The deep aquifer has a much longer delay time for recharge and a much slower recession rate than the shallow aquifer. Parameters for the baseflow filter are also listed in Table 1. It is interesting to notice that using the baseflow days given by the filter program (Arnold et al., 1995, 1999) as the recharge delay time of the deep aquifer reproduced the low-flow very well.

Figure 4 demonstrates comparison of stream flows among the measured and sim-ulated. A five-year clip was took out from the whole simulation period of 39 yr to give a clearer picture. The two-reservoir method improved the low-flow simulation remark-ably in vision. Statistical indices NSE and PBIAS indicate that two-reservoir method yielded "good" or even "very good" results in a sense of either NSE or PBIAS following the rating rules given by Moriasi et al. (2007), which are better than the one-reservoir method, Table 2.

Table 3 lists the summery statistics of measured and simulated streamflow volumes. Annual flow volumes simulated by SWAT using one-reservoir and two-reservoir meth-ods are approximated with only minor differences. The simulated mean annual flow volumes are slightly larger than the measured, and the simulation was rated as very good, Table 2. However, significant differences were found between the simulated and the measured maximum flow volume. The maximum flow volume was observed in 1999, while simulated in 1988. The difference might be due to uncertainty of meteoro-logical input in mountain areas, which was derived from records of the base station at foot of the mountain using a single precipitation lapse rate.

4 Discussion

The annually averaged baseflow volumes given by different approaches were listed in Table 4. The one-reservoir and two-reservoir approaches produced similar results in annual baseflow volumes. The digital filter program gave a much larger baseflow volume than the model-based methods. The model-based baseflow volume accounted for 45 % of the annual flow volume, while the filter-based 60 %. Among the model-based baseflow, shallow aquifer contributed 58 %, and the deep aquifer 42 %. According to the recharge partition coefficient, these should be 60 % and 40 %, respectively. The minor difference was attributed to a portion of the shallow aquifer storage was depleted during the simulation period. For the deep aquifer, its storage fluctuated seasonally while equilibrium was maintained, as the simulation revealed.

The observed streamflow flattens out with delayed flow supply from deeper subsurface stores and eventually become nearly constant, which is sustained by outflow from groundwater storage, Fig. 3. Figure 4 illustrates the baseflow processes. When only one-reservoir was used, the base flow was underestimated as shown in Fig. 4. The observed mean daily flow rate was $9.8\,\mathrm{m}^3\,\mathrm{s}^{-1}$ and the volume of $1.88 \times 10^8\,\mathrm{m}^3$ during the period from October to April, while the simulated value was $3.0\,\mathrm{m}^3\,\mathrm{s}^{-1}$ and the volume of $0.58 \times 10^8\,\mathrm{m}^3$ for the same period. Similar results were also found for Oigaing River basin in Western Tianshan and Ala Archa River basin in Northern Tianshan when a one-reservoir baseflow approach was used (Aizen et al., 2000). The steep slopes of the MRB (Luo et al., 2011, manuscript), the quick recession of surface runoff, and the sluggish and stable baseflow processes during late Autumn and late Spring (Fig. 1) indicate a quick percolation of rainfall and snow and glacier melt waters during the summer time to an underground storage which releases slowly during the winter time, as found by isotopic measurements in the Wind River Range of Wyoming of US (Cable et al., 2011). When the deep aquifer was employed as an additional slow release pool, the baseflow simulation was improved remarkably, as demonstrated in Figs. 5 and 6a, b.

Title Page

Abstract | Introduction

Conclusions | References

Tables | Figures

◄ | ►

◄ | ►

Back | Close

Full Screen / Esc

Printer-friendly Version

Interactive Discussion

The model- and filter-based daily baseflow processes were averaged over the period from 1966 to 1999, Fig. 6. The simulated streamflow peak time seems shift a little earlier. Nevertheless, the simulated rising receding limbs match the measured ones well.

During the low-flow period (from November to April), it was noticed that the one-reservoir method gave a serious underestimation of streamflow, while the two-reservoir method reproduced the streamflow properly. Combination of the quick release reservoir and the slow release reservoir matched both the quick ad sluggish receding stages of recession limb of the streamflow very well. During the quick receding stage, the quick release pool played a more important part than the slow release one, and vice-versa during the sluggish stage, Figs. 3 and 7.

The filter-based baseflow started to rise earlier, reached its peak later, and turns to low-flow stage earlier again than the model-based, Fig. 6. The earlier peak time of the model-based baseflow might be attributed to streamflow peak time shift.

Onset points of rising limbs are worth of notice, Figs. 4 and 6. The filter-based baseflow responds to runoff occurrence immediately at onset of rising limb. The model-based baseflow responds with a delay. The Manas River basin is snow and glacier melt dominated. Snowmelt starts usually in middle of April. Infiltration in frozen soils is affected by soil permeability, water content, repeated thawing and refreezing, and many other factors and their complex interactions (French and Binley, 2004; Stahli, 2005). Experimental (Hayashi et al., 2003; Iwata et al., 2010) and mathematical (Flerchinger and Saxton,1989; Zhao and Gray, 1999) investigation revealed the impeding effects of frozen soil layer to snowmelt infiltration, and hence the potential recharge to aquifers. As a matter of fact, baseflow should respond with a delay to the snowmelt, other than immediately as given by the filter-based approach, Fig. 6. In point view of mathematical simulation, this is achieved by SWAT model through a simple assumption of no water flow during the frozen season. A issue remained to be addressed is infiltration to and recharge from soil profile during freezing and thawing, and eventually determination of the onset point of rising limb, Eqs. (4) and (7). This needs more detailed description to

soil freezing/thawing processes, which are described insufficiently in most watershed hydrological models.

Both the model-based and the filter-based approaches captured the reflection point of recession limb at late September, when direct surface runoff usually ceases to discharge the aquifers.

Compared to one-reservoir, the two-reservoir method requires three extra parameters to calibrate. This case study revealed that the extra parameters will not bring too much extra work for calibration if proper steps are followed. Firstly, calibrate the parameters with recharge to deep aquifer disabled, and optimize parameters with the quick rising and receding limbs as target. Then, activate the recharge to the deep aquifer and optimize the three parameters for the slow release pool. An important reminder is that the slow release pool has a longer recharge delay time and smaller recession constant than the quick release pool. And, as aforementioned, the baseflow days given by the filter-based program can be a tip for calibrating the delay time. The recession constant given by the filter program can also be a initial estimation of recession constant of the slow release pool.

5 Conclusions

In this study we presented a methodology to simulate the baseflow processes by adding a slow reacting linear reservoir to the available quick reacting reservoir of baseflow generation in SWAT model. The baseflow-enhanced SWAT model was used to simulate the streamflow process in the snow and glacier melt dominated Manas River basin in Tianshan Mountains, where the streamflow process is featured with steeper rising and receding limbs from May to September, and quite flatter recession from October to April. Following conclusions were achieved.

Combination of two linear reservoirs achieved the best results in reproducing the streamflow processes. The Nash-Sutcliff efficiency values at the calibration and validation stages are 0.68 and 0.62 for the one-reservoir case, and 0.76 and 0.69 for the two-reservoir case, respectively; percent bias for both cases are better than -4%.

The two-reservoir approach improved the streamflow flow, especially the low-flow remarkably.

The filter-based approach responds immediately to surface runoff occurrence at onset of rising limb, while the model-based approaches with a delay. In consideration of retention of surface storage and impeding effects of frozen soil layers on infiltration during initial snowmelt stage, a delay response is believed more reasonable. Meanwhile, it is suggested that freezing/thawing processes be included in soil modules to determine recharge to the aquifers and hence, the proper timing of baseflow response. The filter- and model-based methods gave similar surface runoff cessation points which are at late September.

The filter-based method estimated the baseflow index as 0.60, while the model-based as 0.45 in the Manas River basin. it cannot be decided which is more representative due to unavailability of baseflow measurements.

References

Aizen, V. B., Aizen, E., Glazirin, G., and Loaiciga, H. A.: Simulation of daily runoff in Central Asian alpine watersheds, J. Hydrol., 238, 15–34, 2000.

Arnold, J. and Allen, P.: Automated methods for estimating baseflow and ground water recharge from streamflow records, J. Am. Water Resour. As., 35, 411–424, 1999.

Arnold, J. and Fohrer. N.: SWAT2000: Current capabilities and research opportunities in applied watershed modeling, Hydrol. Process., 19, 563–572, 2005.

Arnold, J., Allen, P., and Bernhardt, G.: A comprehensive surface-groundwater flow model, J. Hydrol., 142, 47–69, 1993.

Arnold, J., Allen, P., Muttiah, R., and Bernhardt, G.: Automated base flow separation and recession analysis techniques, Ground Water, 33, 1010–1018, 1995.

Arnold, J., Muttiah, R., Srinivasan, R., and Allen, P.: Regional estimation of base flow and groundwater recharge in the upper Mississippi basin, J. Hydrol., 227, 21–40, 2000.

Cable, J., Ogle, K., and Williams, D.: Contribution of glacier melt water to streamflow in the Wind River Range, Wyoming, inferred via a Bayesian mixing model applied to isotopic measurements, Hydrol. Process., 25, 2228–2236, doi:10.1002/hyp.7982, 2011.

Chu, T. W. and Shirmohammadi, A.: Evaluation of the SWAT model's hydrology component in the Piedmont physiographic region of Maryland, Trans. ASAE, 47, 1057–1073, 2004.

Eckhardt, K.: How to construct recursive digital filters for baseflow separation, Hydrol. Process., 19, 507–515, 2005.

Eckhardt, K.: A comparison of baseflow indices, which were calculated with seven different baseflow separation methods, J. Hydrol., 352, 168–173, 2008.

Fenicia, F., Savenije, H. H. G., Matgen, P., and Pfister, L.: Is the groundwater reservoir linear? Learning from data in hydrological modelling, Hydrol. Earth Syst. Sci., 10, 139–150, doi:10.5194/hess-10-139-2006, 2006.

Ferket, B. V. A., Samain, B., and Pauwels, V. R. N.: Internal validation of conceptual rainfall–runoff models using baseflow separation, J. Hydrol., 381, 158–173, 2010.

Flerchinger, G. N. and Saxton, K. E.: Simultaneous heat and water model of a freezing snow-residue-soil system, I. Theory and development, T. ASABE, 32, 565–571, 1989.

French, H. and Binley, A.: Snowmelt infiltration: monitoring temporal and spatial variability using time-lapse electrical resistivity, J. Hydrol., 297, 174–186, 2004.

Hayashi, M., van der Kamp, G., and Schmidt, R.: Focused infiltration of snowmelt water in partially frozen soil under small depressions, J. Hydrol., 270, 214–229, 2003.

Hilberts, A. G. J., van Loon, E. E., Troch, P. A., and Paniconi, C.: The hillslope-storage Boussinesq model for non-constant bedrock slope, J. Hydrol., 291, 160–173, 2004.

Iwata, Y., Hayashi, M., Suzuki, S., Hirota, T., and Hasegawa, S.: Effects of snow cover on soil freezing, water movement, and snowmelt infiltration: a paired plot experiment, Water Resour. Res., 46, W09504, doi:10.1029/2009WR008070, 2010.

Kalin, L. and Hantush, M. H.: Hydrologic modeling of an Eastern Pennsylvania watershed with NEXRAD and rain gauge data, J. Hydrol. Eng., 11, 555–569, 2006.

Luo, Y., Arnold, J., Liu, S. Y., and Wang, X. Y.: Inclusion of Glacier Processes for a Distributed Hydrological Modeling at Basin Scale in Tianshan Mountains, Northwest China, J. Hydrol., under revision, 2011.

Lyne, V. and Hollick, M.: Stochastic time-variable rainfall-funoff modelling, I. E. Aust. Natl. Conf. Publ., 79, 89–93, Inst. of Eng., Aust., Canberra, 1979.

Moriasi, D. N., Arnold, J., Van Liew, M. W., Bingner, R. L., Harmel, R. D., and Veith, T. L.: Model

evaluation guidelines for systematic quantification of accuracy in watershed simulations, T. ASABE, 50, 885–900, 2007.

Nathan, R. J. and MaMahon, T. A.: Evaluation of automated techniques for baseflow and recession analysis, Water Resour. Res., 26, 1465–1473, 1990.

Paniconi, C., Troch, P. A., Emiel van Loon, E., and Hilberts, A. G. J.: Hillslope-storage Boussinesq model for subsurface flow and variable source areas along complex hillslopes: 2. Intercomparison with a three-dimensional Richards equation model, Water Resour. Res., 39, 1317, doi:10.1029/2002WR001730, 2003.

Peterson, J. R. and Hamlet. J. M.: Hydrologic calibration of the SWAT model in a watershed containing fragipan soils, J. Am. Water Resour. As., 34, 531–544, 1998.

Samuel, J., Coulibaly, P., and Metcalfe, R. A.: Identification of rainfall-runoff model for improved baseflow estimation in ungauged basins, Hydrol. Process., online first, doi:10.1002/hyp.8133, 2011.

Srivastava, P., McNair, J. N., and Johnson, T. E.: Comparison of process-based and artificial neural network approaches for streamflow modeling in an agricultural watershed, J. Am. Water Resour. As., 42, 545–563, 2006.

Stahli, M.: Freezing and thawing phenomena in soils, in: Encyclopedia of Hydrological Sciences, vol. 2, edited by: Anderson, M. G., John Wiley, New York, 1069–1076, 2005.

Szilagyi, J.: Sensitivity analysis of aquifer parameter estimations based on the Laplace equation with linearized boundary conditions, Water Resour. Res., 39, 1156, doi:10.1029/2002WR001564, 2003.

Szilagyi, J.: Heuristic continuous base flow separation, J. Hydrol. Eng., 9, 311–318, 2004.

Tallaksen, L. M.: A review of baseflow recession analysis, J. Hydrol., 165, 349–370, 1995.

Troch, P. A., van Loon, A. H., and Hilberts, A. G. J.: Analytical solution of the linearized hillslope-storage Boussinesq equation for exponential hillslope width functions, Water Resour. Res., 40, W08601, doi:10.1029/2003WR002850, 2004.

Wittenberg, H.: Baseflow recession and recharge as nonlinear storage processes, Hydrol. Process., 13, 715–726, 1999.

Wu, K. and Johnston, C. A.: Hydrologic response to climatic variability in a Great Lakes Watershed: a case study with the SWAT model, J. Hydrol., 337, 187–199, 2007.

Zhao, L. and Gray, D. M.: Estimating snowmelt infiltration into frozen soils, Hydrol. Process., 13, 1827–1842, 1999.

Back | Close

Full Screen / Esc

Printer-friendly Version

Interactive Discussion

Table 1. Baseflow parameter values for one reservoir and two reservoir approaches in SWAT and the automated baseflow filter program for Manas River basin, Tianshan, China.

Model	Parameter	unit	Initial value	Calibrated value
One reservoir	$\delta_{gw,sh}$	day	10–30	15
	$\alpha_{gw,sh}$	–	0–1	0.4
	β	–	0	0
Two reservoirs	$\delta_{gw,sh}$	day	10–30	15
	$\alpha_{gw,sh}$	–	0–1	0.4
	$\delta_{gw,dep}$	day	10–300	127
	$\alpha_{gw,dp}$	–	0–1	0.05
	β	–	0–1	0.4
Filter program	λ	–		0.925
	α	–		0.018
	baseflow days	day		127.9

Table 2. The NSE and PBIAS for the simulated discharge by SWAT using one-reservoir and two-reservoir baseflow approaches in the Manas River basin, Tianshan, China.

		NSE	Rating[a]	PBIAS (%)	Rating[a]
One-reservoir	calibration	0.68	Good	−4.0	
	validation	0.62	Satisfactory	−3.5	Very good
	overall	0.65	Good	−3.7	
Two-reservoir	calibration	0.76	Very good	−2.6	
	validation	0.69	Good	−3.6	Very good
	overall	0.72	Good	−3.2	

[a] The rating is based on rules given by Moriasi et al. (2007).

Table 3. Statistical analysis for the baseflow components and index for Manas River basin, Tianshan, Northwest China.

		max	min	mean	stdev
Flow volumes ($10^8 m^3$)	Runoff(M)	20.20	9.36	12.14	2.20
	Runoff(S)-1R	17.64	9.00	12.51	1.83
	Runoff(S)-2R	17.55	9.26	12.52	1.74

Note: Runoff, streamflow; BFL, baseflow; sh, shallow aquifer reservoir; dp, deep aquifer reservoir; filter, filter-based baseflow separation program; 1R, one-reservoir approach; 2R, two-reservoir approach. Baseflow index, proportion of baseflow components of the runoff; SRF, direct surface runoff.

Table 4. Statistical analysis for the baseflow components and baseflow index for Manas River basin, Tianshan, Northwest China.

		max	min	mean	stdev
	BFL-filter	10.71	5.82	7.20	1.11
	BFL-1R	8.10	3.57	5.63	0.87
Flow volumes ($10^8 m^3$)	BFL-2R	8.02	3.81	5.64	0.80
	BFL-sh	4.71	1.94	3.25	0.54
	BFL-dp	3.32	1.87	2.39	0.30
	BFI-Filter	0.64	0.52	0.60	0.03
Baseflow index	BFI-1R	0.51	0.39	0.45	0.03
	BFI-2R	0.50	0.38	0.45	0.03

Fig. 1. A schematic of streamflow components in SWAT model.
Note: P is precipitation; Q_{lt} is lateral soil water flow; S_{sh} and S_{dp} are water storages of the shallow and deep aquifer, respectively; other symbols are mentioned within the text.
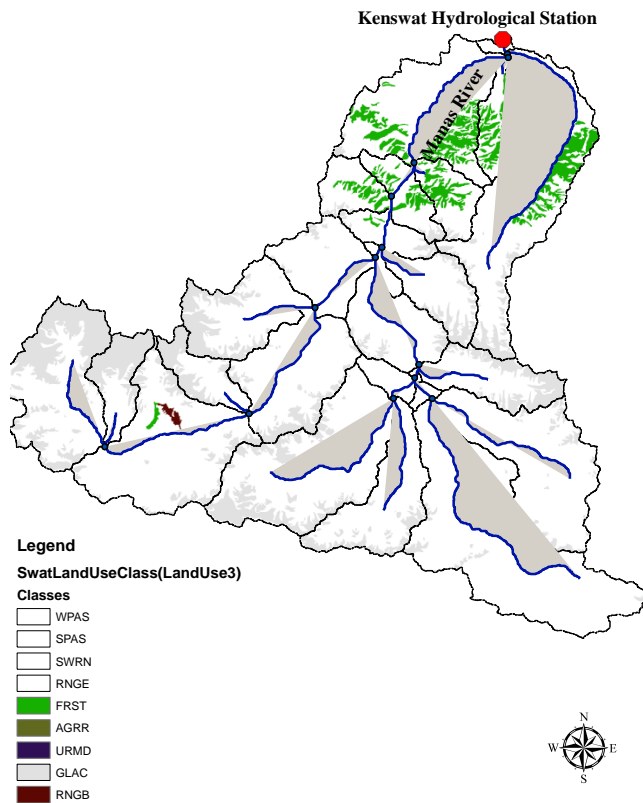
Fig. 2. The Manas River basin and subbasin delineation map.
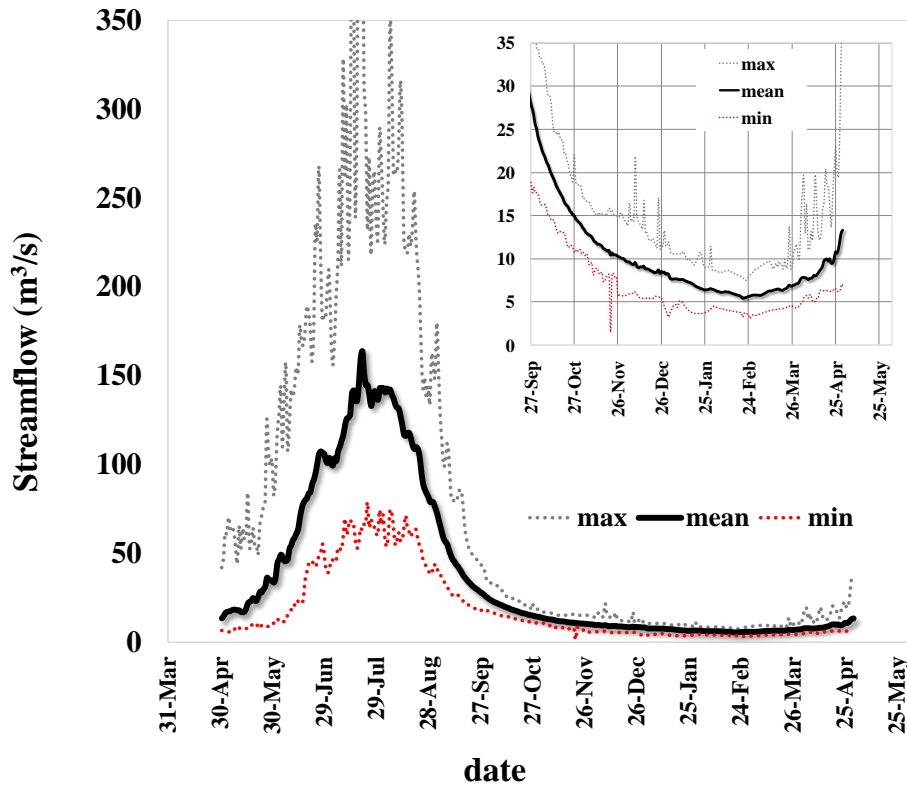
Fig. 3. The measured mean streamflow process of Manas River, Tianshan, Northwest China (max, the maximum daily flow rate; min, the minimum daily flow rate; mean, the mean daily flow rate from 1961 to 1999).

Fig. 4. Comparison of simulated to measured streamflow processes at validation stage, the simulation started in 1961 (ROF, runoff; m, measured; 1R, one-reservoir method; 2R, two-reservoir method).

Full Screen / Esc

Printer-friendly Version

Interactive Discussion
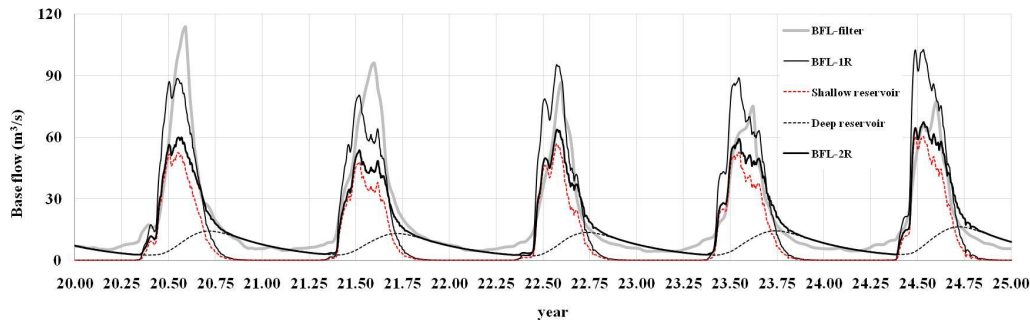
Fig. 5. Clip illustration of the seasonal baseflow processes generated by model- and filter-based approaches, the whole period covered 1961–1999, 1961 as the year 1 (BFL, baseflow; filter, filter-based baseflow separation program; 1R, one-reservoir approach; 2R, two-reservoir approach; Shallow reservoir, the shallow aquifer reservoir generated baseflow; Deep reservoir, the deep aquifer reservoir generated baseflow).
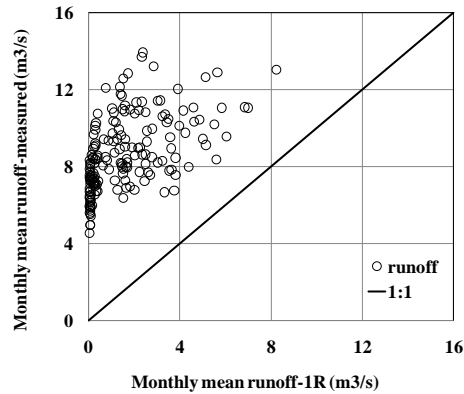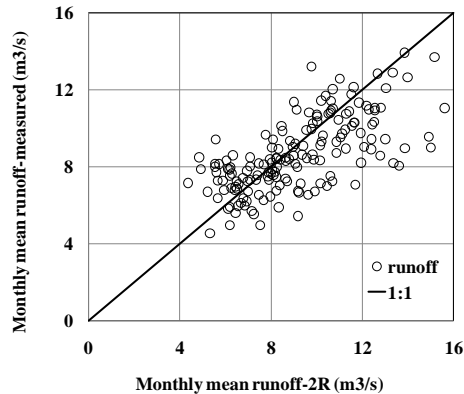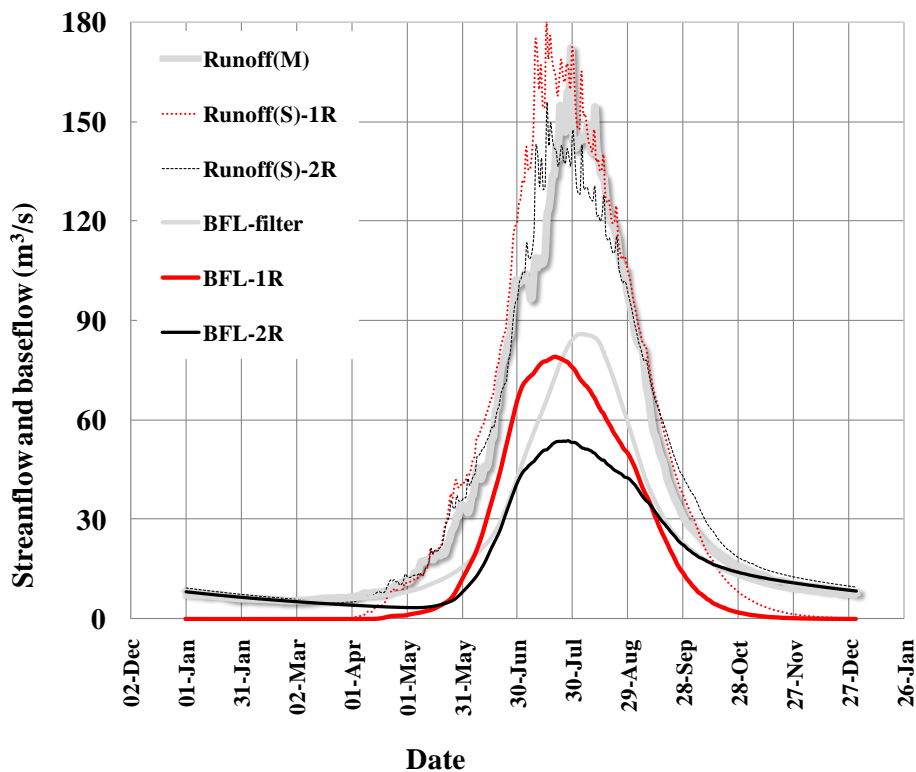
Fig. 6. Comparison of the simulated and measured monthly averaged low-flow discharge rates. **(a)**, the one-reservoir approach was used; **(b)**, the two-reservoir approach was used.

Fig. 7. Comparison of the averaged daily baseflow processes generated by different baseflow approaches (BFL, baseflow; 1R, one-reservoir approach; 1R, two-reservoir approach; filter, filter-based baseflow separation approach).

Title Page

Abstract | Introduction

Conclusions | References

Tables | Figures

Back | Close

Full Screen / Esc

Printer-friendly Version

Interactive Discussion